THE JOURNAL OF PHYSICAL CHEMISTRY B

Article

pubs.acs.org/JPCB

Edelfosine and Miltefosine Effects on Lipid Raft Properties: Membrane Biophysics in Cell Death by Antitumor Lipids

Bruno M. Castro,*[,†] Aleksander Fedorov,[†] Valentin Hornillos,[‡,§] Javier Delgado,[§] A Ulises Acuña,[‡] Faustino Mollinedo,[▽] and Manuel Prieto[†]

[†]Centro de Química Física-Molecular and Institute of Nanoscience and Nanotechnology, IST, Universidade Técnica de Lisboa, Av. Rovisco Pais, 1049-001 Lisboa, Portugal

[‡]Instituto de Química Física Rocasolano, CSIC, Serrano 119, E-28006 Madrid, Spain

[§]Instituto de Química Orgánica General, CSIC, Juan de la Cierva 3, E-28006 Madrid, Spain

[▽]Instituto de Biología Molecular y Celular del Cáncer, Centro de Investigación del Cáncer, CSIC—Universidad de Salamanca, Campus Miguel de Unamuno, E-37007 Salamanca, Spain

Supporting Information

ABSTRACT: Edelfosine (1-*O*-octadecyl-2-*O*-methyl-*sn*-glycero-phosphocholine) and miltefosine (hexadecylphosphocholine) are synthetic alkylphospholipids (ALPs) that are reported to selectively accumulate in tumor cell membranes, inducing Fas clustering and activation on lipid rafts, triggering apoptosis. However, the exact mechanism by which these lipids elicit these events is still not fully understood. Recent studies propose that their mode of action might be related with alterations of lipid rafts biophysical properties caused by these lipid drugs. To achieve a clear understanding of this mechanism, we studied the effects of pharmacologically relevant amounts of edelfosine and miltefosine in the properties of model and cellular membranes. The influence of these molecules on membrane order, lateral organization, and lipid rafts molar fraction and size were studied by steady-state and time-resolved fluorescence methods, Förster resonance energy transfer (FRET), confocal and fluorescence lifetime imaging microscopy (FLIM). We found that the global membrane and lipid rafts biophysical properties of both model and cellular membranes were not significantly affected by both the ALPs. Nonetheless, in model membranes, a mild increase in membrane fluidity induced by both alkyl lipids was detected, although this effect was more noticeable for edelfosine than miltefosine. This absence of drastic alterations shows for the first time that ALPs mode of action is unlikely to be directly linked to alterations of lipid rafts biophysical properties caused by these drugs. The biological implications of this result are discussed in the context of ALPs effects on lipid metabolism, mitochondria homeostasis modulation, and their relationship with tumor cell death.

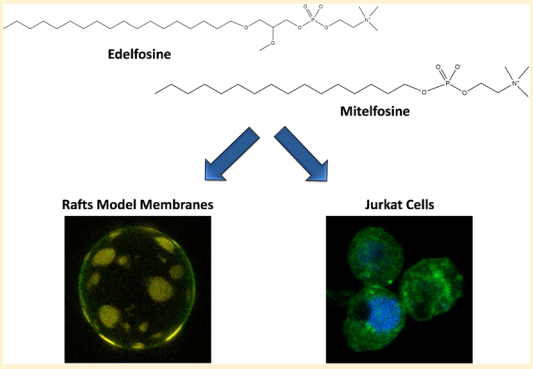

INTRODUCTION

Synthetic alkylphospholipids (ALPs) are promising therapeutic candidates against cancer. Unlike conventional DNA-targeting antineoplastic drugs, these molecules have cell membranes as their primary site of action.[1−3] According to their molecular structure, ALPs comprise two classes (Figure 1): (i) alkyl-lysophospholipids, with the prototypical 1-*O*-octadecyl-2-*O*-methyl-*sn*-glycero-phosphocholine (edelfosine); and (ii) alkyl-phosphocholines, with the prototypical hexadecylphosphocholine (miltefosine). These molecules display selective cytotoxic activity against a wide variety of tumor cells,[4−6] particularly tumors causing hematological malignancies.[7−10] However, their precise mode of action is still largely unknown.

Nowadays, cells membranes are characterized as having distinct lateral assemblies of lipids and proteins that mediate several cellular processes (e.g., sorting and signaling[11,12]). Lipid rafts are membrane regions enriched in cholesterol (Chol) and saturated sphingolipids that are more ordered (liquid-ordered phase, l_o) than the bulk membrane (liquid-disordered phase, l_d).[12] In the past decade, these membrane domains have emerged as important modulators of ALPs' antitumor activity. ALPs are described to accumulate in lipid rafts of several tumor cells, being internalized afterward.[4−9] Raft disruption by Chol depletion agents abrogates ALPs internalization and cell death.[5,6,9,10] Moreover, ALPs modify plasma membrane lipid composition, namely Chol and sphingomyelin content,[3,13] the major constituents of lipid rafts. Edelfosine promotes selective apoptosis in several cancer cells by inducing the coalescence of lipid rafts, which is followed by Fas/CD95 and downstream signaling proteins clustering and activation in those do-

Received: February 7, 2013
Revised: May 22, 2013
Published: June 5, 2013

dx.doi.org/10.1021/jp401407d | *J. Phys. Chem. B* 2013, 117, 7929−7940

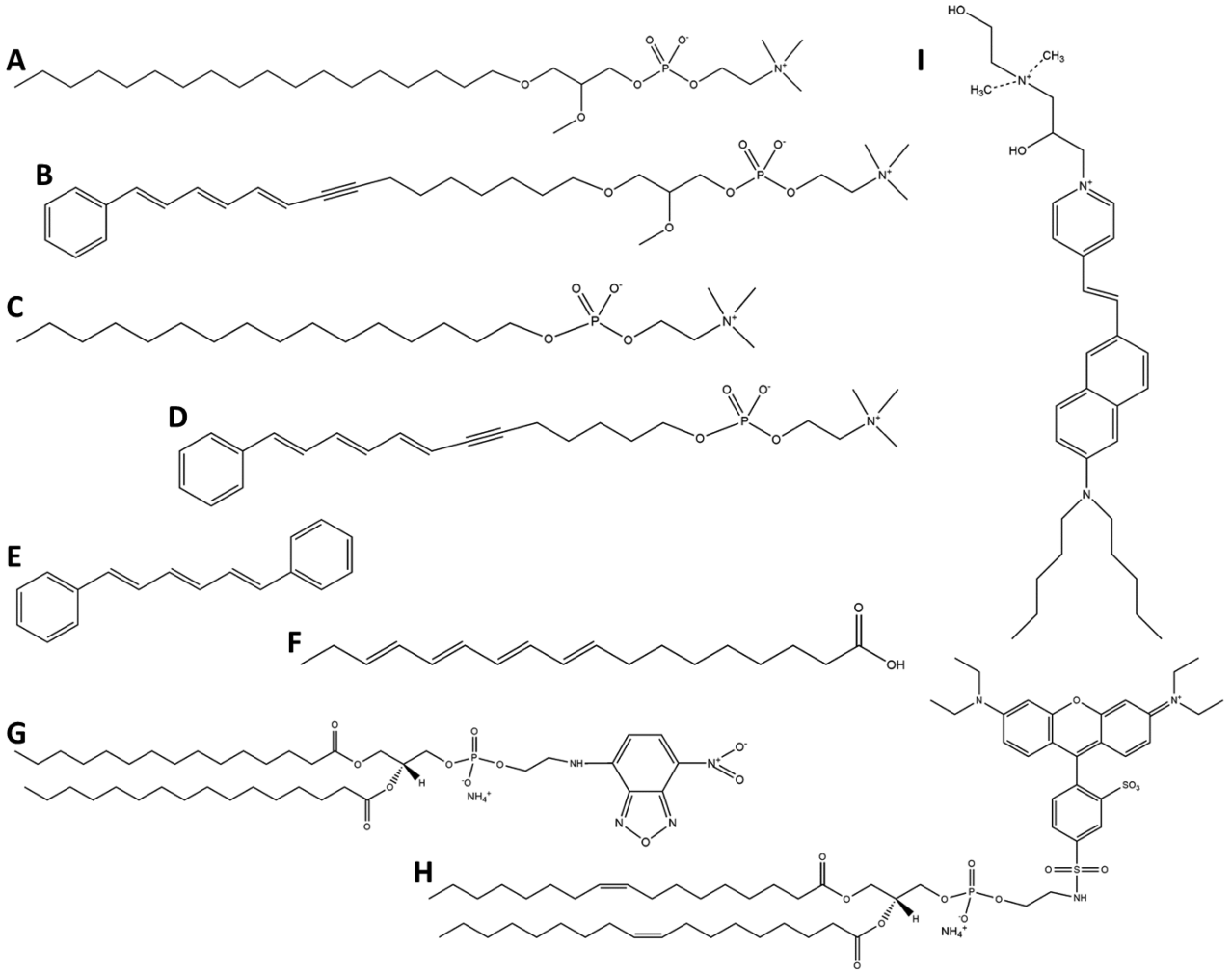

Figure 1. Alkylphospholipids and fluorescent membrane probes used in this study. (A) edelfosine, (B) PTRI-edelfosine, (C) miltefosine, (D) PTRI-miltefosine, (E) DPH, (F) t-PnA, (G) NBD-DPPE, (H) Rho-DOPE, and (I) di-4-ANEPPDHQ.

mains.[4,8,9,14] Similarly, both edelfosine and miltefosine have been shown to decrease lipid rafts order in model membranes.[15−18] Therefore, it seems that the unique biophysical features of lipid rafts are decisive for the cellular outcome of these drugs. In fact, it has been proposed that the mode of action for ALPs might be related to alterations of the plasma membrane, specifically the lipid composition and/or biophysical properties of lipid rafts.[13,15,17] However, a complete understanding of the membrane-associated mechanisms of ALPs-mediated cell death is still lacking. This can only be achieved if the effects of these drugs on membrane and lipid raft properties are known and thoroughly characterized. Only so, a direct cause−effect relationship between the modulation of lipid rafts by these molecules and the recruitment and activation of apoptotic proteins can be attained.

In the present work, we provide a thorough characterization of edelfosine- and miltefosine-induced membrane biophysical alterations on model and cell membranes. A detailed description of the effects of relevant amounts of ALPs at the cellular level (up to 10%)[7−10] on the properties of the raft-model system 1-palmitoyl-2-oleoyl-sn-glycero-3-phosphocholine (POPC)/*N*-palmitoyl-sphingomyelin (PSM)/Chol[19,20] was obtained by combining a multiprobe approach[21−23] and several steady-state and time-resolved fluorescence techniques, including Förster resonance energy transfer (FRET) and confocal microscopy. Fluorescent ALP analogues[24,25] were used to assess and quantify the membrane lateral distribution of the antitumor drugs. Fluorescence lifetime imaging microscopy (FLIM) measurements of Jurkat cells were also performed to assess the in vivo effects of edelfosine on cell membrane properties. Our results show that, in the concentrations studied, edelfosine and miltefosine do not significantly affect the membrane biophysical properties of both model and cell membranes. However, a slight disordering of the membrane, dependent on Chol and ALP's own structure, was detected in membrane model systems. Contrary to what has been proposed, death receptor and downstream apoptotic protein clustering that occurs in the tumor cells of lipid rafts after treatment with ALPs is unlikely to be directly governed by changes of lipid rafts/plasma membrane biophysical properties caused by these drugs. These events are possibly rather indirectly triggered by ALP interferences on membrane lipid metabolism and transport, and/or on intracellular organelle function.

MATERIALS AND METHODS

Materials. The lipids 1-palmitoyl-2-oleoyl-*sn*-glycero-3-phosphocholine (POPC), *N*-palmitoyl-sphingomyelin (PSM), and the probe 1,2-dioleoyl-*sn*-glycero-3-phosphoethanolamine-*N*-(lissamine rhodamine B sulfonyl) (Rho-DOPE) were

dx.doi.org/10.1021/jp401407d | J. Phys. Chem. B 2013, 117, 7929−7940

obtained from Avanti Polar Lipids (Alabaster, AL). Cholesterol (Chol) was from Sigma (St. Louis, MO). The probes 1,2-dipalmitoyl-*sn*-glycero-3-phosphoethanolamine-*N*-(7-nitro-2−1,3-benzoxa-diazol-4-yl) (NBD-DPPE), *trans*-parinaric acid (t-PnA), 1,6-diphenyl-1,3,5-hexatriene (DPH), and di-4-ANEPPDHQ were purchased to Molecular Probes (Leiden, The Netherlands). The alkyl-phospholipid 1-*O*-octadecyl-2-*O*-methyl-*rac*-glycero-phosphocholine (edelfosine) was from R. Berchtold (Biochemisches Labor, Bern, Switzerland) and INKEYSA (Barcelona). Hexadecylphophocholine (miltefosine) was from Calbiochem (San Diego, CA). The fluorescent alkyl ether lipids analogues *all*-(*E*)-1-*O*-(15-phenylpentadeca-10,12,14-triene-8-ynyl)-2-*O*-methyl-*rac*-glycero-3-phosphocholine (PTRI-edelfosine) and *all*-(*E*)-13-phenyltrideca-8,10,12-trien-6-ynylphosphocholine (PTRI-miltefosine) were synthetized as described in refs 24 and 25. All organic solvents were UVASOL grade, from Merck (Darmstadt, Germany), and all of the cell culture chemicals were obtained from Molecular Probes (Leiden, The Netherlands).

Liposome Preparation. Binary POPC/PSM (3.5:1) and ternary multilamellar vesicles (MLV) composed of 14.4:4.6:1, 4.3:1.9:1, 1.8:1.2:1, 1:1:1, 1:1.4:1.6, and 1:2.5:3.2 of POPC/PSM/Chol with or without ether lipid were prepared as previously described.[22] Briefly, lipids, probes and ALPs in the appropriate ratios were mixed from their stock solutions in chloroform, and a dried lipid film was obtained upon evaporation of the organic solvent under a slow stream of N_2. Samples were then left overnight under high vacuum to ensure the evaporation of remaining organic solvent. The mixtures were hydrated with sodium phosphate 10 mM, NaCl 150 mM, EDTA 0.1 mM buffer (pH 7.4), and re-equilibrated by freeze−thaw cycles using liquid nitrogen and a 50 °C water bath. Samples were kept at 4 °C overnight and were slowly brought to room temperature and maintained at this temperature at least for 1 h before the measurements. The probe:lipid ratios used were 1:200 for DPH, PTRI-edelfosine, PTRI-miltefosine, and 1:500 for *t*-PnA. The total lipid concentration was 100 μM and edelfosine and miltefosine content was 0, 5.0, and 10 mol % of the total lipid. The concentrations of lipid and probe stock solutions were determined as previously described.[21] Fluorescent ether lipids analogues stock solution concentration was determined spectrophotometrically using the following *molar absorptivity*(PTRI-edelfosine; PTRI-miltefosine, 345 nm, DMSO): $a = 62.0 \times 10^3$ M^{-1} cm^{-1}.[24,25]

The lipid mixtures studied are contained within the tie-line that spans the liquid-disordered/liquid-ordered (l_d/l_o) phase coexistence region of the POPC/PSM/Chol phase diagram at 23 °C, also enclosing the "canonical raft mixture" (1:1:1) (see Figure S1 in the Supporting Information). The lipid mixtures that lay outside the extremes of the tie-line are, respectively, pure l_d and l_o regions of the phase diagram and were included to better define the variation of the different parameters with the composition of the system. The ternary lipid mixtures chosen have been extensively studied in terms of phase properties and domain size,[19,20] allowing for a good identification of ALPs effects on membrane biophysical features.

Absorption and Fluorescence. All measurements were performed in 0.5 cm × 0.5 cm quartz cuvettes. The absorption and steady-state fluorescence instrumentation was previously described.[26] The absorption spectra were corrected for turbidity. The steady-state fluorescence anisotropy is defined as (see, e.g., ref 27)

$$\langle r \rangle = \frac{(I_{VV} - G \times I_{VH})}{(I_{VV} + 2 \times G \times I_{VH})} \quad (1)$$

in which the different intensities (blank-subtracted) are the steady-state vertical and horizontal components of the fluorescence emission with excitation vertical (I_{VV} and I_{VH}, respectively) and horizontal (I_{HV} and I_{HH}, respectively) to the emission axis. The latter pair of polarized components is used to calculate the *G* factor ($G = I_{HV}/I_{HH}$) that corrects for the differential sensitivity of the emission channel. The excitation/emission ($\lambda_{exc}/\lambda_{em}$) wavelengths were 358 nm/430 nm for DPH, 303 nm/405 nm for t-PnA, and 345 nm/420 nm for the fluorescent ALPs derivatives.

Time-resolved measurements were performed as described in refs 19 and 20. The $\lambda_{exc}/\lambda_{em}$ wavelengths were 295 nm/405 nm for *t*-PnA, 428 nm/536 nm for NBD-DPPE, and 365 nm/440 nm for PTRI-ALPs. The data were analyzed with the TRFA software (Scientific Software Technologies Center, Minsk, Belarus). For a decay described by a sum of exponentials where α_i is the normalized pre-exponential and τ_i is the lifetime of the decay component *i*, the quantum yield-weighted lifetimes ($\overline{\tau}$) and the mean fluorescence lifetime ($\langle\tau\rangle$) are respectively given by

$$\overline{\tau} = \sum_i \alpha_i \tau_i \quad (2)$$

and

$$\langle \tau \rangle = \frac{\sum_i \alpha_i \tau_i^2}{\sum_i \alpha_i \tau_i} \quad (3)$$

Förster Resonance Energy Transfer (FRET) Experiments. FRET experiments were carried out in large unilamellar vesicles (LUV) (1 mM total lipid concentration) prepared from MLV via extrusion, as described previously.[22] The vesicles contained NBD-DPPE/Rho-DOPE as the donor/acceptor pair for FRET between the l_o and l_d phases. The probe/lipid (P/L) ratios used were 1:1000 and 1:200 for donor and acceptor, respectively. For this donor P/L ratio, no donor self-quenching or energy homotransfer takes place.[28] Data analysis was performed as described by de Almeida et al.[20] The FRET efficiency (*E*) was obtained from the time-resolved fluorescence intensity curves, through the relationship $E = 1 - (\overline{\tau}_{DA}/\overline{\tau}_D)$.

Determination of Edelfosine and Miltefosine Fluorescent Analogues Partition Coefficient. The partition coefficient of the edelfosine and miltefosine fluorescent analogues (PTRI-edelfosine and PTRI-miltefosine) between l_o and l_d phases, $K_p^{l_o/l_d}$, in POPC/PSM/Chol ternary mixtures was determined from the variation of their photophysical parameters with the molar fraction of l_o phase (X_{l_o}). The molar fraction of each phase (X_i) was obtained from the tieline of the respective phase diagram (see Figure S1 in the Supporting Information), employing the lever rule. The partition coefficient is an equilibrium constant that quantifies the distribution of the fluorescent drug between the two fluid phases (l_o and l_d) formed in the ternary mixtures. $K_p^{l_o/l_d}$ was calculated according to the following relationships:[22]

dx.doi.org/10.1021/jp401407d | J. Phys. Chem. B 2013, 117, 7929−7940

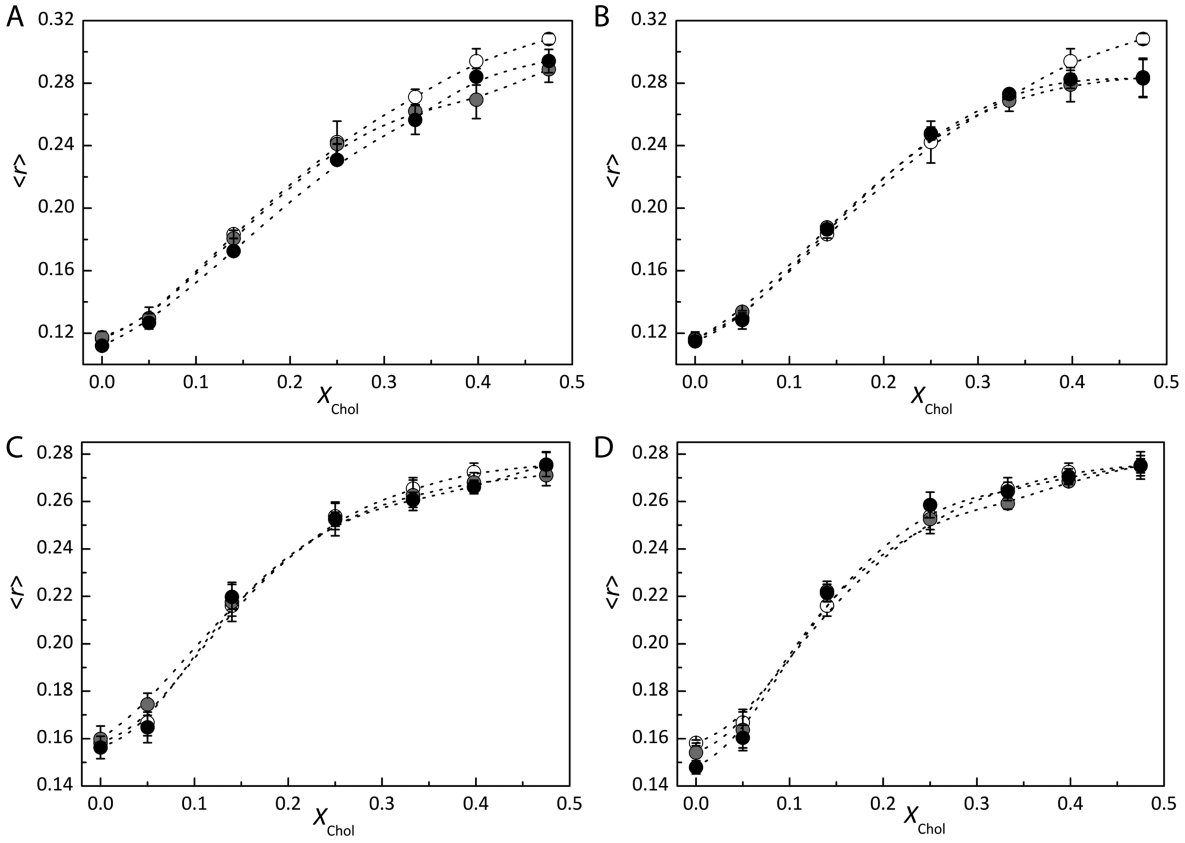

Figure 2. Edelfosine and miltefosine effects on lipid membrane fluidity. Steady-state fluorescence anisotropy ($\langle r \rangle$, eq 1) of (A, B) DPH or (C, D) t-PnA at 23 °C as a function of Chol mole fraction (X_{Chol}) in POPC/PSM/Chol MLV containing 0 (white), 5 (gray) and 10 (black) mol % edelfosine (see panels A and C) or miltefosine (see panels B and D). The error bars are ± the standard deviations of at least three independent samples.

(i) From steady-state fluorescence anisotropy, $\langle r \rangle$:

$$\langle r \rangle = \frac{\varepsilon_{l_o}\phi_{l_o}K_p^{l_o/l_d}\langle r \rangle_{l_o}X_{l_o} + \varepsilon_{l_d}\phi_{l_d}\langle r \rangle_{l_d}X_{l_d}}{\varepsilon_{l_o}\phi_{l_o}K_p^{l_o/l_d}X_{l_o} + \varepsilon_{l_d}\phi_{l_d}X_{l_d}} \quad (4)$$

(ii) From mean fluorescence lifetime, $\langle \tau \rangle$:

$$\langle \tau \rangle = \frac{\langle \tau \rangle_{l_o}K_p^{l_o/l_d}X_{l_o} + \overline{\tau}_{l_d}/\overline{\tau}_{l_o}\langle \tau \rangle_{l_d}X_{l_d}}{K_p^{l_o/l_d}X_{l_o} + \overline{\tau}_{l_d}/\overline{\tau}_{l_o}X_{l_d}} \quad (5)$$

where ε_i is the molar absorption coefficient, ϕ_i is the fluorescence quantum yield, $\langle \tau \rangle_i$ and $\langle r \rangle_i$ are the mean fluorescence lifetime and steady-state fluorescence anisotropy in phase i ($i = l_o$ or l_d), respectively. $K_p^{l_o/l_d}$ is obtained by fitting the equations to the experimental data as a function of X_i.

Confocal Fluorescence Microscopy. Giant unilamellar vesicles (GUVs) composed of POPC/PSM/Chol with or without 10 mol % edelfosine were prepared by electroformation, as described previously.[29] Confocal microscopy was performed using a Leica TCS SP5 inverted microscope (Model DMI6000, Leica Microsystems CMS GmbH, Mannheim, Germany) with a 63× water (1.2 numerical aperture) apochromatic objective. NBD-DPPE (probe/lipid ratio 1/200) and Rho-DOPE (probe/lipid ratio 1/500) excitation was achieved using the 458-nm and the 514-nm lines from the Ar^+ laser, respectively. NBD-DPPE and Rho-DOPE emissions were collected at the wavelength ranges of 530−600 nm and 600−700 nm, respectively.

Cell Culture. The human T-cell leukemia Jurkat cell line was grown in standard RPMI-1640 culture medium supplemented with 10% heat inactivated fetal bovine serum (FBS), 2 mM L-glutamine, 100 U/mL penicillin, and 100 mg/mL streptomycin at 37 °C in humidified 95% air and 5% CO_2.

Fluorescence Lifetime Imaging Microscopy (FLIM). Jurkat cells treated with 10 mM edelfosine for the described times were grown in poly-L-lysine-coated eight-well plates from IBIDI. The cells were then incubated with 5 μM of the fluorescent membrane probe di-4-ANEPPDHQ for 30 min at 37 °C in serum free-medium as described in ref 30. The medium was replaced with Dulbecco's phosphate-buffered saline (DPBS), and cells were imaged at 24 °C for <1 h to ensure their viability.

Microscopy was performed on a Leica TCS SP5 inverted microscope (Model DMI6000, Leica Microsystems CMS GmbH, Mannheim, Germany) with a 63× water (1.2 numerical aperture) apochromatic objective. Probe fluorescence was achieved by two-photon excitation from a pulsed Ti:sapphire laser (Mai Tai BB, Spectra-Physics) with λ_{ex} = 780 nm (100 fs pulse with an 80 MHz repetition rate). Detection was performed using an acoustic-optic beam splitter (AOBS), a 700-nm short pass, and a 500−570 nm emission filters. Fluorescence lifetimes were recorded as a 256 × 256 pixel size image or as the sum of all the image pixels into an average cumulative decay, using SPC v.9.44 acquisition software controlled by a Becker & Hickl SPC-830 TCSPC card (Berlin, Germany). Fluorescence decays were fitted to a two-exponential function using an SPCImage v.3.8.9.0 software package (Becker & Hickl, Berlin, Germany) to obtain the fluorescence lifetime image (threshold = 500 and a binning of 2 × 2 pixels), as described in ref 31. Average cumulative decays

dx.doi.org/10.1021/jp401407d | J. Phys. Chem. B 2013, 117, 7929−7940

were fitted using the TRFA software package (Scientific Software Technologies Center, Minsk, Belarus). For each day of measurement, the instrument response function (IRF) was recorded using urea crystals. This parameter was included in the experimental fitting process for fluorescence lifetime determination.

RESULTS

Edelfosine and Miltefosine Effects on the Biophysical Properties of Raft Model Membranes. We have used the thoroughly characterized mammalian membrane model system POPC/PSM/Chol[19,20] and the fluorescent membrane probes DPH, t-PnA, and NBD-DPPE to obtain a detailed evaluation of edelfosine and miltefosine effects on membrane biophysical properties. The compositions of the selected ternary lipid mixtures lay within the tieline that contains the "canonical" raft mixture (1:1:1), which encompasses membranes presenting a low molar fraction of small l_o domains (rafts) to mixtures with a high molar fraction of large l_o domains.[19,20] In this way, the effects of the two prototypical ALPs on tumor cells membrane before and after treatment, i.e., in membranes presenting small and large rafts, respectively,[7−10] can be mimicked.

Membrane Order and Lipid-Phase Boundaries. To assess edelfosine and miltefosine effects on the membrane order, we have measured DPH, t-PnA, and NBD-DPPE steady-state fluorescence anisotropy, $\langle r \rangle$, on POPC/PSM/Chol MLV, or LUV with or without edelfosine or miltefosine (see Figures 2 and 3). DPH and t-PnA present an even distribution between l_o and l_d phases,[22] and their fluorophores are located in the hydrophobic region of the lipid bilayer. Therefore, their fluorescence properties report the average conformation dynamics of lipids' acyl chains. On the other hand, NBD-DPPE, with its preferential localization into l_o regions ($K_p^{l_o/l_d} \approx 3.5$)[22] and having its fluorophore located near the lipid hydrophilic headgroups/water interface, mainly reports molecular density changes occurring at the lipid−water interface of the membrane-ordered regions.[32] Using this approach, a thorough description of the membrane hydrophobic/hydrophilic and properties of the ordered/disordered regions is obtained.

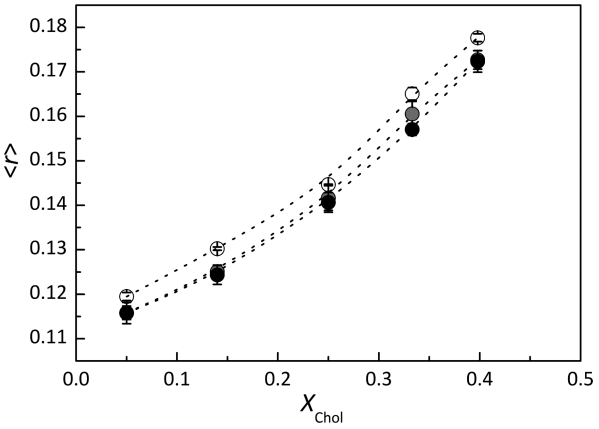

Figure 3. ALPs effects in lipid membrane order. NBD-DPPE steady-state fluorescence anisotropy ($\langle r \rangle$, eq 1) in POPC/PSM/Chol LUV containing 0 (white) and 10 mol % edelfosine (gray) or miltefosine (black) at 23 °C.

From Figure 2, it can be seen that, in the absence of ALPs, DPH and t-PnA anisotropy increase with X_{Chol}, reporting the formation of the l_o phase. When edelfosine or miltefosine are present in the mixtures, the same trend is obtained for both probes. However, although t-PnA anisotropy is largely insensitive to the presence of drugs (see Figures 2C and 2D), DPH anisotropy is mildly affected by the ALPs (see Figures 2A and 2B). Five mole percent (5 mol %) of edelfosine induces a slight decrease in DPH anisotropy in mixtures with high Chol content ($X_{Chol} \geq 0.40$), i.e., membranes in the l_o phase. Doubling the edelfosine concentration to 10 mol % total lipid resulted in a mild but perceptible decrease of DPH anisotropy for mixtures with $X_{Chol} < 0.4$. For membranes in the l_o phase, the decrease of DPH anisotropy caused by this edelfosine concentration was comparable to that obtained for 5 mol % of this ALP (Figure 2A). In the case of miltefosine, a slight decrease on DPH anisotropy was obtained only for membranes in the l_o phase ($X_{Chol} \geq 0.40$) (Figure 2B). However, and analogously to edelfosine, the addition of 5 and 10 mol % of miltefosine to these membranes resulted in similar DPH anisotropy decreases. These results suggest that, in the concentrations used, both edelfosine and miltefosine mildly affect the fluidity of l_o membranes, although this is more noticeable for edelfosine than for miltefosine.

Figure 3 shows the steady-state fluorescence anisotropy of NBD-DPPE as a function of X_{Chol} in POPC/PSM/Chol LUV containing either 10 mol % edelfosine or mitelfosine. In the absence of ALPs, NBD-DPPE anisotropy increases with X_{Chol}, reflecting the formation of a l_o phase. In the presence of 10 mol % edelfosine or miltefosine, the NBD-DPPE anisotropy variation profile is not changed, although it presents lower values for all of the mixtures studied. In this case, edelfosine and miltefosine fluidizing effects are detected for lower X_{Chol}, compared to when t-PnA and DPH were used (see Figure 2). This is a result of NBD-DPPE preferential partition to the l_o phase,[22] meaning that its fluorescent properties are mainly reporting ALP effects on these Chol-enriched regions. DPH and t-PnA, on the other hand, are equally distributed between the l_d and l_o phases, thus reporting the global properties of the membrane, where ALP effects are averaged and consequently attenuated. Hence, NBD-DPPE steady-state anisotropy results show that both edelfosine and miltefosine mainly affect l_o (raft) phase order.

To complement the results obtained from steady-state anisotropy, and to obtain further information on ALPs' ability to change the properties of the lipid phases present in the ternary mixtures studied, time-resolved fluorescence measurements with t-PnA were performed (see Figure 4). t-PnA fluorescence lifetimes have been extremely useful in the detection of lipid domains and in the determination of lipid phase boundaries and phase diagrams (see, e.g., refs 19,21, and 23), because of the high dependence of the nonradiative rate constant of polyene probes on the membrane lipid environment. For all mixtures studied, t-PnA mean fluorescence lifetimes ($\langle \tau \rangle$, eq 3) follow the same trend of variation as the steady-state anisotropy, increasing with X_{Chol}, as a consequence of l_o phase formation (see open symbols in Figure 4). The addition of edelfosine to the ternary mixtures resulted in the shortening of t-PnA mean fluorescence lifetimes, whereas miltefosine inclusion did not cause any significant changes. This is a result of the higher ability of edelfosine to fluidize the membrane, compared to that of miltefosine, as the fluorescence anisotropy data already suggested. Moreover, no dependence of t-PnA mean fluorescence lifetime on edelfosine concentration was detected, in accordance with the steady-state fluorescence

dx.doi.org/10.1021/jp401407d | J. Phys. Chem. B 2013, 117, 7929−7940

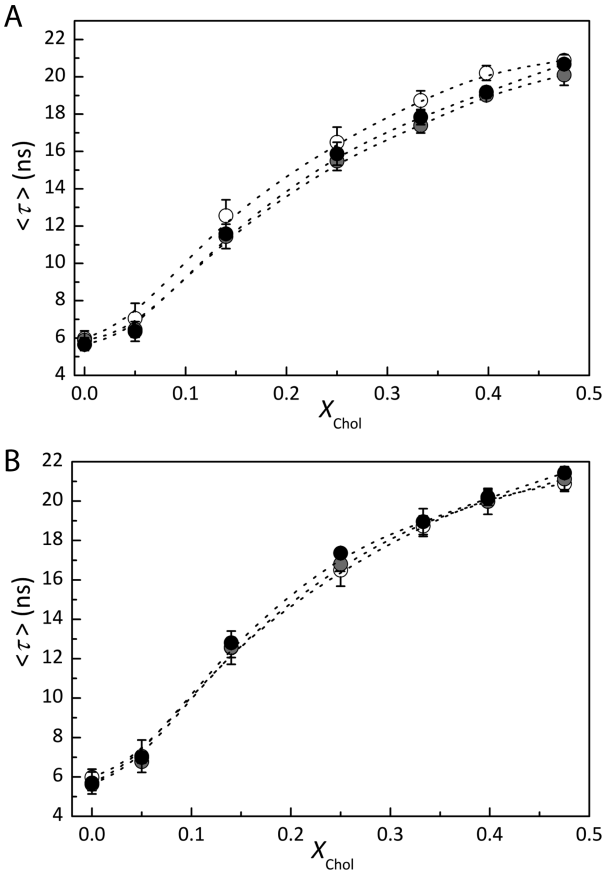

Figure 4. Edelfosine and miltefosine slightly fluidize lipid membranes but do not affect the boundaries of the l_d/l_o coexistence region of the POPC/PSM/Chol phase diagram. Effects of edelfosine (A) or miltefosine (B) in the mean fluorescence lifetime ($\langle r \rangle$, eq 3) of t-PnA at 23 °C in POPC/PSM/Chol MLV containing 0 (white), 5 (gray) and 10 (black) mol % ALP. The error bars are ± the standard deviations of at least three independent samples.

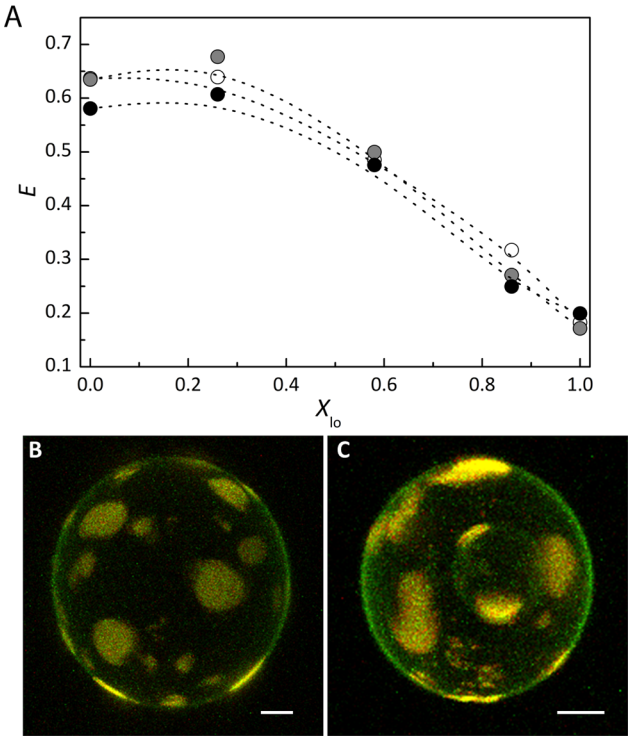

Figure 5. The size distribution of lipid rafts is not affected by edelfosine or miltefosine. (A) Variation of FRET efficiency (E) for the donor/acceptor pair NBD-DPPE/Rho-DOPE as a function X_{lo} in the POPC/PSM/Chol LUV in the absence of edelfosine and miltefosine (white circles), the presence of 10 mol % edelfosine (gray circles), or the presence of miltefosine (black circles). (B, C) Three-dimensional (3D) projection images obtained from confocal sections of GUV labeled with NBD-DPPE (green channel) and Rho-DOPE (red channel) at 23 °C are shown. GUV were prepared from mixtures of PSM/POPC/Chol (1:1:1) (panel B) or of the same lipid mixture containing 10 mol % edelfosine (panel C). (Scale bar = 5 μM.)

results. This shows that the effects of pharmacologically relevant concentrations of edelfosine and miltefosine on membrane fluidity are considerably limited.

The fact that t-PnA mean fluorescence lifetimes in the presence of edelfosine or miltefosine present the same variation as those measured in the absence of drugs demonstrates that neither ALP is affecting the POPC/PSM/Chol phase distribution. Nonetheless, t-PnA shorter fluorescence lifetimes measured in samples containing edelfosine suggest that lipid molecular packing in the l_o phase in the presence of this ALP is different than in its absence.

Lipid Raft Sizes. A lively area of membrane research is related to the size of lipid rafts.[33,34] In membrane model systems, both nanoscopic and micrometer-sized domains have been shown to coexist.[20] Usually, nanoscopic domains are detected and characterized using spectroscopic techniques (fluorescence, nuclear magnetic resonance (NMR) and electron spin resonance (ESR)), whereas micrometer-sized domains are studied by microscopy methods.[33] To evaluate possible effects of edelfosine and miltefosine on the different size ranges of the lipid domains formed in the POPC/PSM/Chol "raft" mixtures, FRET and confocal microscopy experiments were performed (Figure 5). The FRET efficiency (E) between a donor and acceptor that preferentially localize into distinct lipid phases can be used to estimate the sizes of lipid domains in the nanometer scale.[20] In this study, the donor/acceptor pair NBD-DPPE/Rho-DOPE was used, since these probes preferentially localize into l_o and l_d domains, respectively.[22] The results obtained for POPC/PSM/Chol LUV in the absence and presence of 10 mol % edelfosine or miltefosine, as a function of X_{l_o} are presented in Figure 5A. Neither of the two drugs induced significant changes in the FRET efficiency between the probes. In the low X_{l_o} regime, the FRET efficiency is high, indicating that both donor and acceptor are relatively close to each other at a distance not much larger than the Förster radius ($R_0 \sim 50$ Å). Since the two probes are preferentially located in different lipid phases (either l_d or l_o), domain sizes should be small (<20 nm).[20] For higher X_{l_o}, the FRET efficiency decreases because of the formation of larger l_o domains (25−100 nm),[20] causing a greater separation of the two probes.

To assess the effects of edelfosine on l_o domain sizes in the micrometer range, fluorescence confocal microscopy images of POPC/PSM/Chol GUV with or without 10 mol % edelfosine and labeled with NBD-DPPE and Rho-DOPE were obtained (see Figures 5B and 5C). The green and red detection channels of the microscope were used to acquire NBD-DPPE and Rho-DOPE emission, respectively. Because of the distinct partition and quantum yield of the probes in l_d and l_o phases, in the microscopy images, l_d domains are seen as round yellowish

dx.doi.org/10.1021/jp401407d | J. Phys. Chem. B 2013, 117, 7929−7940

regions whereas l_o domains are recognized as green areas. Edelfosine did not induce any substantial changes in the size distribution of the macroscopic domains, nor did it induce any notable changes in the fractional amount of each phase, in agreement with the fluorescence spectroscopy results (Figure 4A, invariance of the phase boundaries) and the above FRET data (Figure 5A). However, this ALP decreased the stability of the POPC/PSM/Chol vesicles, causing the GUVs to burst within 30−60 min after their formation (see Video 1 in the Supporting Information). This is probably due to the formation of edelfosine micelles that might destabilize the GUV structure. In the electroformation of GUVs, a relatively high lipid concentration (~1.0 mM) is required. Thus, 10 mol % edelfosine will correspond to a total drug concentration of ~100 μM, which is well above the value of its critical micelle concentration (CMC = 19.0 μM).[35] Consequently, edelfosine micelles may form, causing the observed GUV destabilization.

Edelfosine and Miltefosine Membrane Lateral Distribution. To determine the lipid phase preference (l_d vs l_o) of edelfosine and miltefosine in the ternary mixtures studied, the ALP fluorescent analogues PTRI-edelfosine and PTRI-miltefosine were used. These molecules preserve the amphipathic properties, the main structural motifs, the proapoptotic activity, and also the intracellular localization of their parent nonfluorescent counterparts.[24,25] The steady-state anisotropy and fluorescence lifetimes of these fluorescent lipids were measured in mixtures contained along the tie-line that encompasses the 1:1:1 lipid composition in l_d/l_o phase coexistence region of the POPC/PSM/Chol phase diagram (see Figure S1 in the Supporting Information). The fluorescence properties of the ALP analogues were observed to be moderately sensitive to the formation of the l_o phase (see Figure 6), compared to membrane probes such as DPH and t-PnA (compare Figure 1 vs Figure 3). In pure l_d membranes (X_{l_o} = 0), the steady-state fluorescence anisotropy and mean lifetimes of both fluorescent lipids present low values. In membranes displaying l_d/l_o phase coexistence, the fluorescence parameters of both ALP derivatives increase with X_{l_o}, reaching their maximum value in pure l_o membranes. From this variation, and taking into account their photophysical properties in pure l_d and l_o phase, it is possible to determine the partition coefficient of both edelfosine and miltefosine fluorescent analogues between the l_d and l_o phases in the ternary lipid mixtures, $K_p^{l_o/l_d}$, from the fit of eqs 4 and 5 to the experimental data. The results obtained either from steady-state anisotropy or fluorescence lifetimes (Table 1) are similar and show that, in this ternary lipid system, both fluorescent ALP have a marked preference for "non-raft" membrane regions (l_d). In Figure 6 are also presented the steady-state anisotropy and mean fluorescence lifetime variation curves expected for PTRI-edelfosine if it presented a strong (favorable) partition for the l_o phase (see Figure 6 for further details). Note the contrasting variation profiles between the experimental and theoretical curves.

Edelfosine Effects on the Membrane Order of Jurkat Cells. As shown above, edelfosine has a more noticeable membrane disordering effect than miltefosine. Therefore, we sought to investigate if this ALP would have the same outcome when inserted in the plasma membrane of living cells. We used Jurkat cells, which represent a leukemia cell line that is sensitive to edelfosine treatment[7,8] and, hence, are a good candidate for this type of study. Jurkat cells were incubated with edelfosine

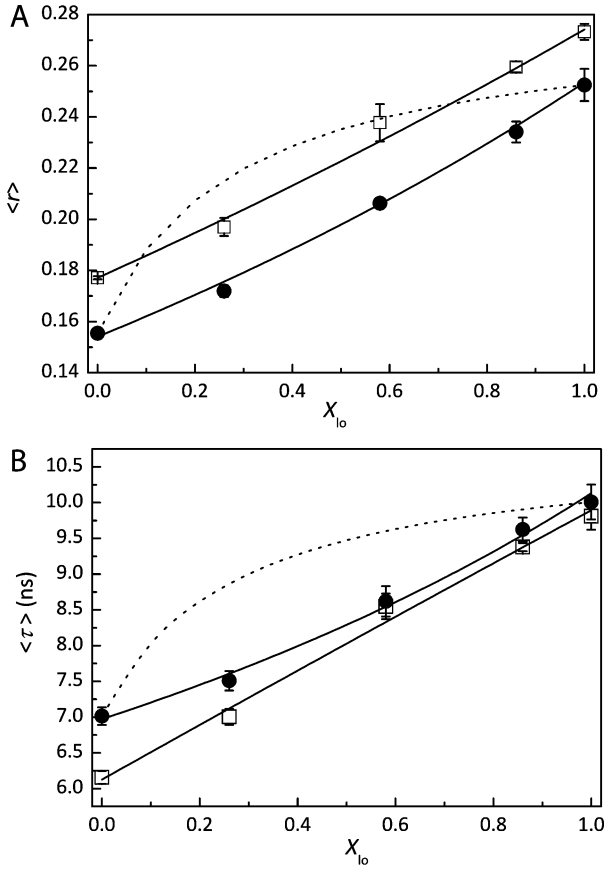

Figure 6. The fluorescent analogues of edelfosine and miltefosine are able to detect l_o phase formation and their photophysical parameters allow the determination of their l_o/l_d partition coefficient ($K_p^{l_o/l_d}$). (A) Steady-state anisotropy or (B) mean fluorescence lifetime of PTRI-edelfosine (black circles) and PTRI-miltefosine (open squares) in MLV contained within the l_d/l_o tieline of the POPC/PSM/Chol phase diagram, as a function of X_{l_o} at 23 °C. The error bars are ± the standard deviations of at least three independent samples, and the solid lines are the nonlinear fit of eqs 4 and 5, with the $K_p^{l_o/l_d}$ values presented in Table 1. The dotted line in panels A and B respectively represent the expected PTRI-edelfosine steady-state anisotropy and mean fluorescence lifetime theoretical variation in the case where the probe presented a favorable partition toward the l_o phase ($K_p^{l_o/l_d}$ = 3). These were calculated according to eqs 4 and 5 and $\overline{\tau}_{l_d}$ = 5.84 ns and $\overline{\tau}_{l_o}$ = 10 ns.

Table 1. Partition Coefficients of PTRI-Edelfosine and PTRI-Miltefosine between l_o and l_d Phases ($K_p^{l_o/l_d}$) in POPC/PSM/Chol Mixtures

	$K_p^{l_o/l_d}$		
ALP	⟨r⟩ (eq 4)	⟨r⟩ (eq 5)	average
PTRI-edelfosine	0.514 ± 0.082	0.463 ± 0.096	0.489 ± 0.178
PTRI-miltefosine	0.488 ± 0.077	0.563 ± 0.111	0.526 ± 0.188

for different times, and their membrane order was measured using the fluorescent membrane probe di-4-ANEPPDQH. The fluorescence wavelength and lifetime of this probe are sensitive to the lipid bilayer order. It has been reported that, between l_d and l_o, its emission presents a 60-nm blue shift and its fluorescence lifetime increases by ~1700 ps.[31,36] For these reasons, this probe has been used to study lipid order of both model and cell membranes,[30,31,36] including plasma membrane

dx.doi.org/10.1021/jp401407d | J. Phys. Chem. B 2013, 117, 7929−7940

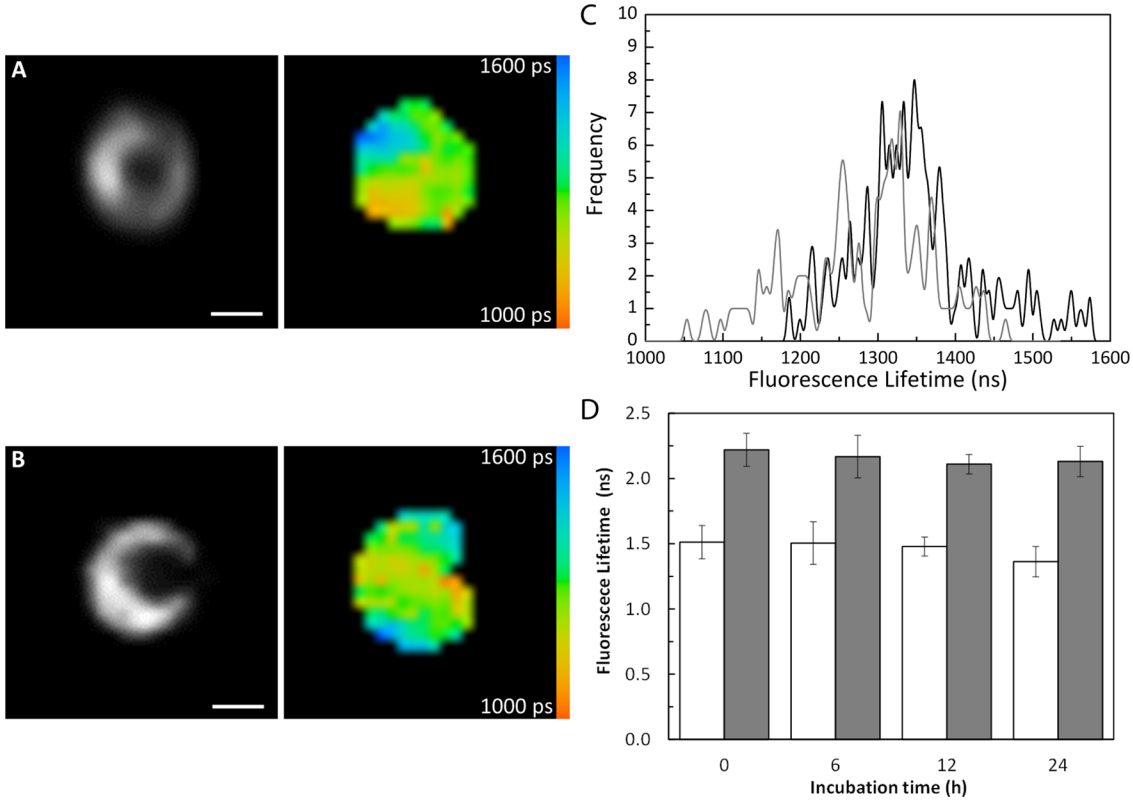

Figure 7. Edelfosine does not significantly affect the plasma membrane order of live Jurkat cells. Representative two-photon fluorescence intensity and fluorescence lifetime microscopy (FLIM) images of Jurkat cells labeled with di-4-ANEPPDHQ (A) before and (B) after treatment with 10 μM edelfosine for 12 h (bar = 5 μm). (C) Fluorescence lifetime (eq 2) histograms of the FLIM images in panel A (black) and panel B (gray). (D) Mean of the average cumulative fluorescence lifetimes of Jurkat cells labeled with di-4-ANEPPDHQ, as a function of incubation time calculated according to eq 2 (white bars) or eq 3 (gray bars). A minimum of five independent measurements were used in the calculations.

order alterations that occur during the formation of the immunological synapse in Jurkat cells.[37] Using fluorescence lifetime imaging microscopy (FLIM), we measured di-4-ANEPPDHQ fluorescence lifetimes in Jurkat cells treated with edelfosine. Representative fluorescence intensity and lifetime images of Jurkat cells labeled with this probe before and after 12 h of treatment with 10 μM edelfosine are shown in Figure 7. Also shown are the fluorescence lifetime histograms for those images and the average cumulative fluorescence lifetimes of Jurkat cells labeled with this probe for the different incubations times studied (see the Materials and Methods section for further details). From these measurements, it can be concluded that edelfosine does not cause drastic changes in the fluorescence lifetime of di-4-ANEPPDHQ. This result shows that edelfosine treatment does not significantly affect the order of the Jurkat cells' plasma membrane, even after 24 h of incubation with the drug. Although at large incubation times, the fluorescence lifetime of di-4-ANEPPDHQ becomes shorter, this is likely due to the plasma membrane destabilization that is characteristic of apoptotic cells. It is known that ~35% of Jurkat cells are already undergoing apoptosis after 24 h of incubation with edelfosine.[4]

DISCUSSION

The lateral organization of membrane lipids into specific domains and the cellular roles carried/mediated by these regions is currently a central topic in cell biology.[11,12] Several active molecules, both intrinsic and extrinsic, exploit the particular molecular environment of these lipid domains to exert their biological functions. The antineoplastic activity of the prototypical ALPs edelfosine and miltefosine is intimately related with lipid rafts,[4−9] although its mode of action is still not fully understood. It has been proposed that the modulation of the biophysical properties of lipid rafts by these molecules could be the mechanism by which these molecules trigger apoptosis.[13,15,17] This study focused on the effects caused by these drugs on the biophysical properties of lipid rafts in order to clarify the link between these alterations and ALPs' biological action. We have followed an experimental strategy where a detailed description of edelfosine and miltefosine effects on lipid rafts properties of a well-studied raft-model was complemented with studies in living cells. This method allowed us to identify the specific effects of the two drugs on membrane biophysical features, which otherwise would not be possible in the complex molecular environment of cell membranes. At the same time, these studies facilitate the interpretation of the drugs' in vivo effects. Hence, a comprehensive description of ALP effects on the biophysical properties of the membranes of live cells could be attained.

Edelfosine and Miltefosine Weakly Modify Lipid Ordering in Model Raft Membranes while Preserving Domain Size Distribution. Our results show that pharmacologically relevant concentrations of edelfosine and miltefosine[7−10] cause a slight decrease of the lipid acyl chain order of model raft membranes. These results are in agreement with those obtained for higher concentrations of these alkyl lipids gathered from other physical techniques, including calorimetry, X-ray diffraction, and NMR spectroscopy or fluorescence

dx.doi.org/10.1021/jp401407d | J. Phys. Chem. B 2013, 117, 7929−7940

quenching.[15−18] Nonetheless, none of these studies comment about the different membrane disordering abilities of the two ALPs. Here, we demonstrate that the membrane fluidizing extent of edelfosine and miltefosine depend on both ALP structure and membrane Chol concentration. Although edelfosine is able to mildly decrease the membrane order of all lipid mixtures studied, miltefosine membrane disordering effects were only detected for mixtures with high Chol fractional concentration ($X_{Chol} \geq 0.40$) (see Figures 2 and 4). This is further shown by the edelfosine- and miltefosine-induced decrease of NBD-DPPE steady-state anisotropy (Figure 3), a probe that preferentially partitions to the l_o phase[22] and thus mainly reports the effects of ALPs on those domains. For pure l_o membranes, an increase of ALPs concentration did not correlate with an increase in membrane fluidity, as seen from DPH and t-PnA steady-state anisotropy (Figure 2). This result suggests that in the concentrations studied, edelfosine and miltefosine ability to disorder the membrane is quite limited.

Edelfosine is distinguished from miltefosine by the presence of a glycerol moiety.[3] Nevertheless, this structural motif does not interfere with the way these two molecules interact with Chol, since studies in lipid monolayers have shown that both edelfosine and miltefosine strongly interact with Chol and in a similar way.[38,39] Therefore, it is unlikely that their distinct ability for membrane disordering reflects dissimilarities in their interaction with Chol, but rather differences in the membrane molecular arrangement imposed by edelfosine glycerol moiety. The methyl group present at the *sn*-2 position of the edelfosine molecule might somewhat hinder the formation of tight interactions between this ether lipid and other membrane lipid molecules, resulting in a less-ordered lipid environment.

Despite this mild membrane fluidizing effect, neither edelfosine nor miltefosine affect the boundaries of the POPC/PSM/Chol diagram (Figure 4). This results shows that the composition of the l_d and l_o phases is not significantly altered by these molecules. However, the lower mean fluorescence lifetime values of t-PnA in pure l_o mixtures ($X_{Chol} \geq 0.40$) with edelfosine (Figure 5A) demonstrates that the membrane lipid molecular arrangement is slightly changed, as already discussed. Since this ether lipid does not affect the biophysical properties of membranes in the l_d phase (Figure 5A, mixtures with $X_{Chol} = 0$ and 0.05), nor the lipid phase diagram, the shortening of the t-PnA mean fluorescence lifetime is reporting a specific decrease caused by the drug in l_o phase order. Therefore, in the presence of edelfosine, lipids in the l_o phase display slightly greater conformational freedom. Because of the preferential interactions of edelfosine with Chol,[39,40] it is reasonable to assume that the lower order of the l_o phase is a result of that process. An estimate of the number of Chol molecules that interact with edelfosine in a pure l_o phase (mixture with $X_{Chol} = 0.40$) can be obtained by assessing the loss of Chol molecules interacting with PSM. From the decrease in t-PnA mean fluorescence lifetimes caused by edelfosine, using eq 5 and the photophysical parameters of t-PnA in pure l_d and l_o phases ($\overline{\tau}_{l_d} = 3.7$ ns, $\overline{\tau}_{l_o} = 12.6$ ns and $K_p^{l_o/l_d} = 0.88$),[22] it is possible to translate the decrease in the probe mean fluorescence lifetime induced by edelfosine into a decrease in the amount of l_o phase (X_{l_o}) in a mixture without drug. This value can then be converted to X_{Chol}, by employing the lever rule to the tieline of the POPC/PSM/Chol phase diagram. The decrease in membrane order induced by either 5 or 10 mol % edelfosine can be attributed to an estimated decrease in ∼6 mol % of total Chol. This means that, on average, each edelfosine molecule interacts with ∼1 Chol molecule, which is in good agreement with the 1:1 stoichiometry reported for lysophosphatidylcholine and edelfosine interaction with this sterol.[39,41]

A trademark of ALPs-induced cell death is raft coalescence into regions enriched in apoptotic proteins.[4,8,9,14] We have used FRET and confocal microscopy (Figure 5) to study if edelfosine and miltefosine change lipid domain size in POPC/PSM/Chol membranes. Our results show that neither ALP significantly change the size of the l_o domains formed in this mixtures in both nanometer and micrometer length scales. Furthermore, no significant changes in the l_o phase fraction between GUVs with and without edelfosine were observed (Figure 5B), in agreement with fluorescence spectroscopy data (Figure 4, invariance of lipid phase boundaries). As discussed further ahead, alterations of plasma membrane lipid composition caused by these drugs might be underneath this process.

Because of their amphiphilic structure, edelfosine and miltefosine have a potent surfactant activity, forming micelles in aqueous media in the low micromolar concentration range. It could be argued that, in the present study, some of the membrane disordering effects caused by these drugs might result from micelle formation. However, several factors tend to minimize this effect: (i) the ALPs where cosolubilized in organic solvent with the other lipids and upon hydration are readily incorporated into the lipid bilayer; (ii) in the lipid mixtures where the effects of these drugs are more pronounced, large amounts of Chol are present. In this situation, and since ALPs have a strong affinity for Chol,[38,39] which is inserted in the bilayer, it is highly unlikely that ALPs assume a different organization other than being embedded within the bilayer; (iii) the membrane solubilization (detergent) effect of these ALPs is rather low, because of their small CMC values;[35,42] (iv) mixed micelle formation induced by edelfosine was only detected for 20 mol % of the drug[15] (in the present work, the highest edelfosine concentration studied was 10 mol %, which is well below that concentration); and (v) if micelles were in fact formed, resulting to some extent in bilayer solubilization, it would be expected that the photophysical parameters of the membrane probes would be affected due to probe incorporation into those structures. However, no evidence for micelle formation is obtained from the fluorescence properties of the probes. Therefore, the probes are indeed reflecting edelfosine and miltefosine properties when embedded within a fluid lipid bilayer.

In a very recent study, Gomide et al.[43] using GUV composed of a 1:1:1 mixture of 1,2-dioleoyl-sn-glycero-3-phosphocholine (DOPC), sphingomyelin, and Chol showed that the ALPs 10-(octyloxy) decyl-2-(trimethylammonium) and perofosine induce a rapid lipid and domain redistribution, followed by vesicle disruption. These results are contrary to those reported here and can be attributed to the following factors:

(i) *ALP concentration.* In most of our studies, we used ALP concentrations that fit within their pharmacologically relevant range (≤10 μM).[7−10] Gomide et al.[43] used 100 μM solutions of both ALPs. Certainly at this concentration, edelfosine and miltefosine will also induce drastic alterations of membrane properties, as supported by the GUV bursting mediated by edelfosine mentioned above (see Video 1 in the Supporting Information).

(ii) *Structure of the ALPs*. In this study, we show that the effect of ALPs on membrane properties is dependent on their own structure (higher fluidizing effect of edelfosine, compared to miltefosine). Gomide et al.[43] studied two ALPs structurally distinct from those studied here. These might interact differently with the lipid membrane and thus display stronger disordering/destabilizing abilities than edelfosine and miltefosine;

(iii) *Membrane lipid composition*. Gomide et al.[43] used GUV-composed DOPC/bovine brain sphingomyeline/Chol instead of the POPC/PSM/Chol membranes studied here. Although unlikely, ALPs might interact differently with the lipids present in both mixtures, and this could somehow potentiate their disordering effects.

Edelfosine Does Not Perturb the Lipid Order of Plasma Membrane of Jurkat Cells. The FLIM data clearly shows that the overall order of the plasma membrane of Jurkat cells is not affected by edelfosine. Cell membranes are composed of a huge variety of lipids and proteins and, hence, have slightly different properties from those of model membranes composed of simple mixtures of lipids. As shown here, edelfosine disordering effect is more pronounced for membranes in a pure l_o phase or containing high X_{l_o}. Given the intrinsic fluidity of cellular membranes and lipid domains, edelfosine mild fluidizing effects will not be very pronounced on these structures. Furthermore, edelfosine has been described to establish favorable interactions with membrane components not present in the model membranes studied, namely gangliosides,[16] which might further attenuate these effects. For miltefosine, although in vivo measurements were not performed, a similar result is expected. The effects of this phosphocholine in model membranes are comparable to those of edelfosine. Moreover, and as mentioned above, the fact that miltefosine interacts with other membrane components in a manner comparable to that for edelfosine[38,39] supports the expectation that these two ALPs will have analogous effects in cellular plasma membranes.

From these results, it is improbable that lipid raft coalescence and Fas and downstream apoptotic proteins clustering and activation observed after ALP treatment[4,8,9,14] are a direct consequence of the effect of ALPs on the biophysical properties of the membrane. These are rather likely to be indirect consequences of ALP-mediated alterations on other cellular features/processes. These drugs have been shown to inhibit phosphatidylcholine synthesis in the endoplasmatic reticulum,[3,13] and to interfere with cholesterol ester synthesis, markedly decreasing Chol transport from the plasma membrane and increasing Chol biosynthesis.[13] These certainly affect cell membrane lipid composition, which might lead to the coalescence of Fas-enriched lipid rafts and subsequent activation. Similarly, it has been recently shown that ALPs accumulate in mitochondria, causing their swelling and destabilization.[24,44] These intracellular organelles are vital components of cell's apoptosis machinery, and their deterioration and subsequent apoptosis initiation might be a direct result of ALPs effects on mitochondrial membranes. These issues are however beyond the scope of the present work and will be addressed in future studies.

Edelfosine and Miltefosine Fluorescent Analogues Preferentially Localize into Disordered Membrane Regions. In vivo studies with several tumor cell types have shown that edelfosine localizes into lipid rafts.[4−9] To determine if this membrane lateral behavior was a result of its preferential insertion into the special molecular environment of rafts and exclusive to edelfosine, we have studied the partition of the two ALPs fluorescent analogues between l_o and l_d phases formed in POPC/PSM/Chol mixtures. This could be performed (i) because the POPC/PSM/Chol phase diagram is not affected by neither ALP (as discussed above), (ii) because a tie-line for this phase diagram was previously estimated[19] (see Figure S1 in the Supporting Information), and finally (iii) due to the availability of fluorescent edelfosine and miltefosine analogues (PTRI derivatives),[24,25] whose photophysical parameters change with the amount of l_o phase (Figure 6). Interestingly, the low l_o/l_d partition coefficients obtained for both fluorescent ALP (Table 1) indicate that their relative concentration in l_d (non-raft) regions is ∼2 times higher than that of l_o (raft) ones. Since, in vivo, these fluorescent ALPs display the same proapoptotic activity and intracellular localization as their respective parent drugs,[24,25] it is very likely that they will also present a similar membrane lateral distribution. It can thus be concluded that, in membranes containing l_d/l_o phase coexistence, as it is proposed to occur in cellular plasma membrane,[11,12] edelfosine and miltefosine will present a preferential localization into more disordered regions. These results are slightly different from those obtained in previous study where a similar edelfosine fluorescent analogue was reported to distribute equally between l_o and l_d phases.[45] The most significant structural differences between the two probes besides the fluorescent groups (a conjugated phenyltetraene instead of a phenyltriene) is perhaps the fact that the fluorescent phenyltetraene-edelfosine used in that study is much more flexible than the phenyltriene-edelfosine used here, and it can adopt an extended *all-trans* conformation that should fit better among the well-aligned lipid chains, which is a typical feature of ordered lipid phases. Furthermore, the lipid composition of the system used on that study is different from the one studied here, and, therefore, the lipid phases formed on both systems may have distinct properties.

The results obtained for the fluorescent ALPs analogues used in this study are in accordance with the favorable insertion of ALPs into disordered lipid membranes, compared to ordered ones.[15,40] These data show that the in vivo accumulation of these drugs in lipid rafts cannot be explained solely by favorable interactions with Chol molecules,[38,39] since these are not strong enough to overcome the energetic costs faced when inserting these molecules into the ordered raft phase. This conclusion is further supported by the observation that binary edelfosine/Chol liposomes, when used as drug delivery vectors, show low hemolytic side effects while still preserving edelfosine apoptotic properties.[46] If edelfosine accumulation in lipid rafts were uniquely a result of its preferential interaction with Chol, the drug will remain associated with the sterol in vector liposomes, rather than be delivered to the tumor cells. In vivo, other process(es) must facilitate ALPs incorporation into lipid rafts. It has been recently suggested that glangliosides, which are a lipid species that is elevated in the plasma membrane of tumor cells,[47,48] may play a role in edelfosine localization to lipid rafts.[16] Edelfosine presents a strong affinity for gangliosides, establishing stable interactions which are thermodynamically more favorable than edelfosine interactions with raft SM. The more fluid environment of cellular lipid rafts, compared to those of model membranes,[49] might be another factor contributing for ALP accumulation in lipid rafts regions of cellular membranes. Hence, ALP in vivo incorporation into

cellular lipid rafts might be more favorable than in model membranes.

CONCLUSIONS

Lipid rafts and Chol have an important role in alkylphospholipids (ALPs) uptake and cell killing.[5,6,9,10] In the pharmacologically relevant concentration range, edelfosine and miltefosine do not significantly affect the biophysical properties of lipid rafts, which hypothetically could facilitate Fas recruitment and clustering in those regions.[50] These results show, for the first time, that the ALPs mechanism of action are unlikely to be related to the effects of these molecules on the biophysical properties of mammalian plasma membranes and/or lipid rafts, contrary to what has been previously proposed.[13,15,17] ALP-mediated cell death is possibly associated with their role regarding the metabolism and transport of membrane lipids[3,13] and/or intracellular organelles such as mitochondria.[9,24,44] This study, by narrowing the array of processes believed to be responsible for ALPs mode of action, constitutes an important contribution for the elucidation of this still elusive event.

ASSOCIATED CONTENT

Supporting Information

An additional figure and video are available as Supporting Information. This information is available free of charge via the Internet at http://pubs.acs.org.

AUTHOR INFORMATION

Corresponding Author

*Tel.: +34 935542232. Fax: +34 935534000. E-mail: bruno.castro@icfo.es.

Present Address

B.M.C.: ICFO—The Institute of Photonic Sciences, Av. Carl Friedrich Gauss, Num. 3, 08860 Castelldefels (Barcelona), Spain.

Notes

The authors declare no competing financial interest.

ACKNOWLEDGMENTS

We gratefully acknowledge the late Prof. F. Amat-Guerri for his dedicated teaching and guidance in the synthesis of the fluorescent analogues of edelfosine and miltefosine. This work was supported by Grant Nos. PTDC/QUI-BIQ/099947/2008, PTDC/QUI-BIQ/112067/2009, and PTDC/QUI-BIQ/119494/2010, and fellowship BD/36635/2007 (B.M.C.) from Fundação para a Ciência e Tecnologia, Portugal and by project CTQ/2010/16457 (A.U.A.) from Ministerio de Ciencia e Innovación, Spain.

REFERENCES

(1) Gajate, C.; Mollinedo, F. Biological activities, mechanisms of action and biomedical prospect of the antitumor ether phospholipid ET-18-OCH(3) (edelfosine), a proapoptotic agent in tumor cells. *Curr. Drug Metab.* **2002**, *3* (5), 491−525.

(2) Mollinedo, F. Antitumour ether lipids: Proapoptotic agents with multiple therapeutic indications. *Exp. Opin. Ther. Pat.* **2007**, *17* (4), 385−405.

(3) van Blitterswijk, W. J.; Verheij, M. Anticancer alkylphospholipids: Mechanisms of action, cellular sensitivity and resistance, and clinical prospects. *Curr. Pharm. Des.* **2008**, *14* (21), 2061−2074.

(4) Gajate, C.; Gonzalez-Camacho, F.; Mollinedo, F. Involvement of raft aggregates enriched in Fas/CD95 death-inducing signaling complex in the antileukemic action of edelfosine in Jurkat cells. *PLoS One* **2009**, *4* (4), e5044.

(5) van der Luit, A. H.; Budde, M.; Ruurs, P.; Verheij, M.; van Blitterswijk, W. J. Alkyl-lysophospholipid accumulates in lipid rafts and induces apoptosis via raft-dependent endocytosis and inhibition of phosphatidylcholine synthesis. *J. Biol. Chem.* **2002**, *277* (42), 39541−39547.

(6) Vink, S. R.; van der Luit, A. H.; Klarenbeek, J. B.; Verheij, M.; van Blitterswijk, W. J. Lipid rafts and metabolic energy differentially determine uptake of anti-cancer alkylphospholipids in lymphoma versus carcinoma cells. *Biochem. Pharmacol.* **2007**, *74* (10), 1456−1465.

(7) Gajate, C.; Mollinedo, F. The antitumor ether lipid ET-18-OCH(3) induces apoptosis through translocation and capping of Fas/CD95 into membrane rafts in human leukemic cells. *Blood* **2001**, *98* (13), 3860−3863.

(8) Gajate, C.; Del Canto-Janez, E.; Acuna, A. U.; Amat-Guerri, F.; Geijo, E.; Santos-Beneit, A. M.; Veldman, R. J.; Mollinedo, F. Intracellular triggering of Fas aggregation and recruitment of apoptotic molecules into Fas-enriched rafts in selective tumor cell apoptosis. *J. Exp. Med.* **2004**, *200* (3), 353−365.

(9) Gajate, C.; Gonzalez-Camacho, F.; Mollinedo, F. Lipid raft connection between extrinsic and intrinsic apoptotic pathways. *Biochem. Biophys. Res. Commun.* **2009**, *380* (4), 780−784.

(10) Mollinedo, F.; de la Iglesia-Vicente, J.; Gajate, C.; Estella-Hermoso de Mendoza, A.; Villa-Pulgarin, J. A.; Campanero, M. A.; Blanco-Prieto, M. J. Lipid raft-targeted therapy in multiple myeloma. *Oncogene* **2010**, *29* (26), 3748−3757.

(11) Simons, K.; Gerl, M. J. Revitalizing membrane rafts: New tools and insights. *Nat. Rev. Mol. Cell Biol.* **2010**, *11* (10), 688−699.

(12) Lingwood, D.; Simons, K. Lipid rafts as a membrane-organizing principle. *Science* **2010**, *327* (5961), 46−50.

(13) Jimenez-Lopez, J. M.; Rios-Marco, P.; Marco, C.; Segovia, J. L.; Carrasco, M. P. Alterations in the homeostasis of phospholipids and cholesterol by antitumor alkylphospholipids. *Lipids Health Dis.* **2010**, *9*, 33.

(14) Gajate, C.; Mollinedo, F. Edelfosine and perifosine induce selective apoptosis in multiple myeloma by recruitment of death receptors and downstream signaling molecules into lipid rafts. *Blood* **2007**, *109* (2), 711−719.

(15) Ausili, A.; Torrecillas, A.; Aranda, F. J.; Mollinedo, F.; Gajate, C.; Corbalan-Garcia, S.; de Godos, A.; Gomez-Fernandez, J. C. Edelfosine is incorporated into rafts and alters their organization. *J. Phys. Chem. B* **2008**, *112* (37), 11643−11654.

(16) Hac-Wydro, K.; Dynarowicz-Latka, P. Searching for the role of membrane sphingolipids in selectivity of antitumor ether lipid-edelfosine. *Colloids Surf., B* **2010**, *81* (2), 492−497.

(17) Heczkova, B.; Slotte, J. P. Effect of anti-tumor ether lipids on ordered domains in model membranes. *FEBS Lett.* **2006**, *580* (10), 2471−2476.

(18) Alonso, L.; Mendanha, S. A.; Marquezin, C. A.; Berardi, M.; Ito, A. S.; Acuna, A. U.; Alonso, A. Interaction of miltefosine with intercellular membranes of stratum corneum and biomimetic lipid vesicles. *Int. J. Pharm.* **2012**, *434* (1−2), 391−398.

(19) de Almeida, R. F.; Fedorov, A.; Prieto, M. Sphingomyelin/phosphatidylcholine/cholesterol phase diagram: Boundaries and composition of lipid rafts. *Biophys. J.* **2003**, *85* (4), 2406−2416.

(20) de Almeida, R. F.; Loura, L. M.; Fedorov, A.; Prieto, M. Lipid rafts have different sizes depending on membrane composition: A time-resolved fluorescence resonance energy transfer study. *J. Mol. Biol.* **2005**, *346* (4), 1109−1120.

(21) Castro, B. M.; de Almeida, R. F.; Silva, L. C.; Fedorov, A.; Prieto, M. Formation of ceramide/sphingomyelin gel domains in the presence of an unsaturated phospholipid: A quantitative multiprobe approach. *Biophys. J.* **2007**, *93* (5), 1639−1650.

(22) Silva, L. C.; de Almeida, R. F.; Castro, B. M.; Fedorov, A.; Prieto, M. Ceramide-domain formation and collapse in lipid rafts: Membrane reorganization by an apoptotic lipid. *Biophys. J.* **2007**, *92* (2), 502−516.

(23) Castro, B. M.; Silva, L. C.; Fedorov, A.; de Almeida, R. F.; Prieto, M. Cholesterol-rich fluid membranes solubilize ceramide domains: Implications for the structure and dynamics of mammalian intracellular and plasma membranes. *J. Biol. Chem.* **2009**, *284* (34), 22978−22987.
(24) Mollinedo, F.; Fernandez, M.; Hornillos, V.; Delgado, J.; Amat-Guerri, F.; Acuna, A. U.; Nieto-Miguel, T.; Villa-Pulgarin, J. A.; Gonzalez-Garcia, C.; Cena, V.; Gajate, C. Involvement of lipid rafts in the localization and dysfunction effect of the antitumor ether phospholipid edelfosine in mitochondria. *Cell Death Dis.* **2011**, *2*, e158.
(25) Saugar, J. M.; Delgado, J.; Hornillos, V.; Luque-Ortega, J. R.; Amat-Guerri, F.; Acuna, A. U.; Rivas, L. Synthesis and biological evaluation of fluorescent leishmanicidal analogues of hexadecylphosphocholine (miltefosine) as probes of antiparasite mechanisms. *J. Med. Chem.* **2007**, *50* (24), 5994−6003.
(26) de Almeida, R. F.; Loura, L. M.; Fedorov, A.; Prieto, M. Nonequilibrium phenomena in the phase separation of a two-component lipid bilayer. *Biophys. J.* **2002**, *82* (2), 823−834.
(27) Lakowicz, J. R. *Principles of Fluorescence Spectroscopy*; Springer: New York, 2006.
(28) Loura, L. M.; Fedorov, A.; Prieto, M. Fluid−fluid membrane microheterogeneity: A fluorescence resonance energy transfer study. *Biophys. J.* **2001**, *80* (2), 776−788.
(29) Pinto, S. N.; Silva, L. C.; de Almeida, R. F.; Prieto, M. Membrane domain formation, interdigitation, and morphological alterations induced by the very long chain asymmetric C24:1 ceramide. *Biophys. J.* **2008**, *95* (6), 2867−2879.
(30) Owen, D. M.; Rentero, C.; Magenau, A.; Abu-Siniyeh, A.; Gaus, K. Quantitative imaging of membrane lipid order in cells and organisms. *Nat. Protoc.* **2012**, *7* (1), 24−35.
(31) Owen, D. M.; Lanigan, P. M.; Dunsby, C.; Munro, I.; Grant, D.; Neil, M. A.; French, P. M.; Magee, A. I. Fluorescence lifetime imaging provides enhanced contrast when imaging the phase-sensitive dye di-4-ANEPPDHQ in model membranes and live cells. *Biophys. J.* **2006**, *90* (11), L80−L82.
(32) Chattopadhyay, A.; London, E. Parallax method for direct measurement of membrane penetration depth utilizing fluorescence quenching by spin-labeled phospholipids. *Biochemistry* **1987**, *26* (1), 39−45.
(33) Goni, F. M.; Alonso, A.; Bagatolli, L. A.; Brown, R. E.; Marsh, D.; Prieto, M.; Thewalt, J. L. Phase diagrams of lipid mixtures relevant to the study of membrane rafts. *Biochim. Biophys. Acta* **2008**, *1781* (11−12), 665−684.
(34) Munro, S. Lipid rafts: Elusive or illusive? *Cell* **2003**, *115* (4), 377−388.
(35) Busto, J. V.; Sot, J.; Goni, F. M.; Mollinedo, F.; Alonso, A. Surface-active properties of the antitumour ether lipid 1-*O*-octadecyl-2-*O*-methyl-rac-glycero-3-phosphocholine (edelfosine). *Biochim. Biophys. Acta* **2007**, *1768* (7), 1855−1860.
(36) Jin, L.; Millard, A. C.; Wuskell, J. P.; Clark, H. A.; Loew, L. M. Cholesterol-enriched lipid domains can be visualized by di-4-ANEPPDHQ with linear and nonlinear optics. *Biophys. J.* **2005**, *89* (1), L04−L06.
(37) Owen, D. M.; Oddos, S.; Kumar, S.; Davis, D. M.; Neil, M. A.; French, P. M.; Dustin, M. L.; Magee, A. I.; Cebecauer, M. High plasma membrane lipid order imaged at the immunological synapse periphery in live T cells. *Mol. Membr. Biol.* **2010**, *27* (4−6), 178−189.
(38) Gomez-Serranillos, I. R.; Minones, J., Jr.; Dynarowicz-latka, P.; Miniones, J.; Iribarnegaray, E. Miltefosine-cholesterol interactions: A monolayer study. *Langmuir* **2004**, *20* (3), 928−933.
(39) Więcek, A.; Dynarowicz-Łątka, P.; Miñones, J., Jr.; Conde, O.; Casas, M. Interactions between an anticancer drug—edelfosine—and cholesterol in Langmuir monolayers. *Thin Solid Films* **2008**, *516* (24), 8829−8833.
(40) Hac-Wydro, K.; Dynarowicz-Latka, P.; Wydro, P.; Bak, K. Edelfosine disturbs the sphingomyelin-cholesterol model membrane system in a cholesterol-dependent way—The Langmuir monolayer study. *Colloids Surf., B* **2011**, *88* (2), 635−640.
(41) Van Echteld, C. J.; De Kruijff, B.; Mandersloot, J. G.; De Gier, J. Effects of lysophosphatidylcholines on phosphatidylcholine and phosphatidylcholine/cholesterol liposome systems as revealed by ^{31}P-NMR, electron microscopy and permeability studies. *Biochim. Biophys. Acta* **1981**, *649* (2), 211−220.
(42) Rakotomanga, M.; Loiseau, P. M.; Saint-Pierre-Chazalet, M. Hexadecylphosphocholine interaction with lipid monolayers. *Biochim. Biophys. Acta* **2004**, *1661* (2), 212−218.
(43) Gomide, A. B.; Thomé, C. H.; dos Santos, G. A.; Ferreira, G. A.; Faça, V. M.; Rego, E. M.; Greene, L. J.; Stabeli, R. G.; Ciancaglini, P.; Itri, R. Disrupting membrane raft domains by alkylphospholipids. *Biochim. Biophys. Acta* **2013**, *1828* (5), 1384−1389.
(44) Kuerschner, L.; Richter, D.; Hannibal-Bach, H. K.; Gaebler, A.; Shevchenko, A.; Ejsing, C. S.; Thiele, C. Exogenous ether lipids predominantly target mitochondria. *PLoS One* **2012**, *7* (2), e31342.
(45) Bakht, O.; Delgado, J.; Amat-Guerri, F.; Acuna, A. U.; London, E. The phenyltetraene lysophospholipid analog PTE-ET-18-OMe as a fluorescent anisotropy probe of liquid ordered membrane domains (lipid rafts) and ceramide-rich membrane domains. *Biochim. Biophys. Acta* **2007**, *1768* (9), 2213−2221.
(46) Busto, J. V.; Del Canto-Janez, E.; Goni, F. M.; Mollinedo, F.; Alonso, A. Combination of the anti-tumour cell ether lipid edelfosine with sterols abolishes haemolytic side effects of the drug. *J. Chem. Biol.* **2008**, *1* (1−4), 89−94.
(47) Kaucic, K.; Etue, N.; LaFleur, B.; Woods, W.; Ladisch, S. Neuroblastomas of infancy exhibit a characteristic ganglioside pattern. *Cancer* **2001**, *91* (4), 785−793.
(48) Segui, B.; Andrieu-Abadie, N.; Jaffrezou, J. P.; Benoist, H.; Levade, T. Sphingolipids as modulators of cancer cell death: Potential therapeutic targets. *Biochim. Biophys. Acta* **2006**, *1758* (12), 2104−2120.
(49) Kaiser, H. J.; Lingwood, D.; Levental, I.; Sampaio, J. L.; Kalvodova, L.; Rajendran, L.; Simons, K. Order of lipid phases in model and plasma membranes. *Proc. Natl. Acad. Sci. U.S.A.* **2009**, *106* (39), 16645−16650.
(50) Castro, B. M.; de Almeida, R. F.; Goormaghtigh, E.; Fedorov, A.; Prieto, M. Organization and Dynamics of Fas Transmembrane Domain in Raft Membranes and Modulation by Ceramide. *Biophys. J.* **2011**, *101* (7), 1632−1641.